Ion-selective membranes for the recovery of ammonium and potassium

Casadella Muni, Anna

Chapter 5

Ammonium across a selective polymer inclusion membrane: characterization, transport and selectivity

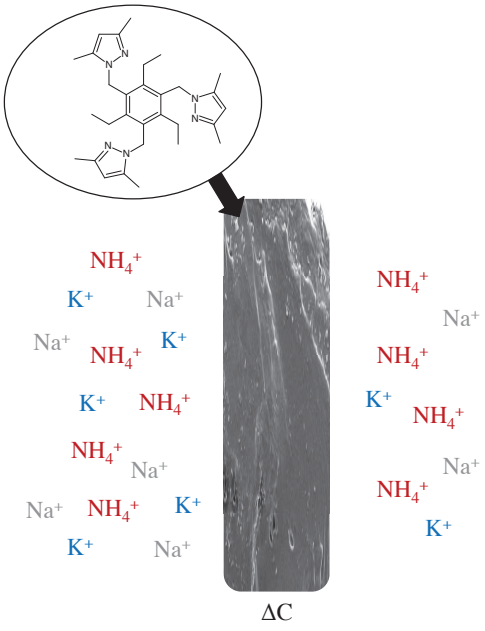

Abstract

The recovery of ammonium from urine requires a system that can distinguish and exclude the competitive ions (sodium and potassium). We developed a polymer inclusion membrane selective for ammonium using an ionophore based on tripodal pyrazole substituted benzene. We studied the interactions of each of the components and their effect on the membrane transport and selectivity in the presence of competitive cations. Spectroscopic and thermogravimetric measurements showed no extensive physical interactions of all components (hydrogen bonding, ionic interactions etc.) and that the plasticizer reduces the rigidity of the membrane by reducing the intermolecular forces among the polymer groups. The addition of ionophore turned the membrane more rigid although it increased its swelling degree and therefore the affinity of the cations to the membrane. A weight ratio of plasticizer (DEHP) and polymer (PVC) of 1:3 resulted in the highest ammonium flux. The two tested contents of ionophore (2 and 5 wt.%) showed that the higher the content of ionophore in the membrane matrix, the fastest the flux is (7.5 $x10^{-3}$mmol $cm^{-2} \cdot h^{-1}$). However, selectivity of NH_4^+ over Na^+ and over K^+ is reduced from 13.07 to 9.33 and from 14.15 to 9.57 correspondingly.

Keywords: ammonium; polymer inclusion membrane; characterization; ion transport; selectivity

---

This Chapter has been **accepted** in *Macromolecular Rapid Communications (MRC)* (2016).
Authors: A. Casadellà, O. Schaetzle, K. Loos.

5.1 Introduction

The population on our planet is experiencing a significant growth and so is the need for food production (i.e., crops). This fact will require higher crop yields [1] and the application of fertilizers either natural (e.g. manure) or synthetic. Nowadays, the production of fertilizers depends on scarce resources [2] and/or energy intensive processes [3]. For a more sustainable approach for the production of fertilizers, recent studies are focusing on exploiting wastewater, such as urine, as an alternative resource [2, 4-6]. In urine, the main cations are: sodium (Na^+), potassium (K^+), ammonium (NH_4^+) [7]. Ammonium is an essential nutrient for plant growth and its economical separation and recovery from urine has raised much interest in biological systems [8-10]. However, its recovery requires a system that can distinguish and exclude the competitive ions. In the case of urine, the competitive cations for NH_4^+ are K^+ and Na^+ because they have the same valence (+1), similar hydrated radii [11] and diffusion coefficient [12]. Therefore, charge, size and mobility are not suitable parameters for the separation and recovery of ammonium.

In literature numerous studies can be found that show the possibility to recover cations, anions and organic molecules using solvent extraction as well as the transport through liquid membranes (LMs) [13-16]. However, LMs present poor stability and flux and membrane technology evolved towards polymer inclusion membranes (PIMs) [17, 18]. PIMs can separate and recover small organic molecules from an aqueous mixture as well as transport metal ions with high selectivity and flux. For instance, Schow *et al.* [19] observed that the flux of a PIM was three orders of magnitude higher than for a supported liquid membrane (SLM) under the same conditions. PIMs are composed of polymer, plasticizer and carrier [17], the same composition as the membranes in ion-selective electrodes (ISEs) [20, 21]. Polymers provide mechanical strength to the membrane; the most common polymers for PIMs and ISE are cellulose

triacetate (CTA) and poly(vinyl chloride) (PVC) due to their high solubility in organic solvents. Plasticizers are generally used to increase the ion flux across the membrane and to provide flexibility to the membrane. Carriers have a specific host-guest complexation behavior which allows the transport (PIMs) or electric signal (ISEs) of the target ion.

Most literature on ammonium-selective carriers is found around ISEs due to the relevance of the π – ammonium ion interaction in the biochemical community [22]. Until recently, the most commonly employed carrier was nonactin, a natural antibiotic [23]. However, its selectivity for NH_4^+ over K^+ is not satisfactory to be practical for artificial membranes. Therefore, studies have focused on the synthesis of carriers with higher selectivity. A vast variety of ionophores has been developed: crown ethers [24], cryptates (water soluble) [25], tripodal pyrazole substituted benzenes [26-28], thiazolebenzo-crown ethers [29], 19-membered-crown rings with bulky subunits [23], cyclodepsipeptides [30], bicyclic peptides [31], etc. These ionophores have selectivity for NH_4^+ over Na^+ and K^+ comparable or higher than nonactin. Yet, the steps required for their synthesis do not make these ionophores economically competitive for their application in ammonium-selective PIMs and further up-scaling. Only the synthetic route of tripodal pyrazole substituted benzenes is short and simple and provides relative high yields (>60%), which makes this molecule a good candidate for development of ammonium-selective PIMs.

In this research we develop a polymer inclusion membrane selective for ammonium using tripodal pyrazole substituted benzene as the ionophore. The interactions of each of the components and their effect on the membrane transport and selectivity in the presence of competitive cations is reported.

5.2 Experimental

5.2.1 Chemicals

Potassium nitrate (KNO_3), sodium nitrate ($NaNO_3$), ammonium nitrate (NH_4NO_3), 3,5-dimethylpyrazole (Scheme 1, B), sodium hydride (NaH) (60% dispersion in mineral oil), anhydrous tetrahydrofuran (THF), 1,3,5-tris(bromomethyl)-2,4,6-triethylbenzene (Scheme 1, A), chloroform ($CHCl_3$), deuterated chloroform ($CDCl_3$) magnesium sulfate ($MgSO_4$), diethyl ether, polyvinyl chloride (PVC), bis(2-ethylhexyl)adipate (DEHP) were purchased from Sigma Aldrich. All chemicals (highest purity grade) were used without further purification except the oil around NaH that was washed away with diethyl ether. Aqueous solutions were prepared using ultrapure water obtained by a Millipore purification unit.

5.2.2 Synthesis of the ionophore

Scheme 1 shows the synthetic route for a tripodal ionophore based on tripodal pyrazole substituted benzene in positions 1, 3 and 5 by pyrazole-based compounds already reported by Chin *et. al.* [26, 27]. To 40mL of anhydrous THF containing a suspension of NaH (0.62g, 16mmol) was added 3,5-dimethhylpyrazole (Scheme 1, B) (1.46g, 16mmol) in small amounts at room temperature. The mixture was stirred for 20min while hydrogen gas was released. The mixture was then slowly added to a slurry of 1,3,5-tris(bromomethyl)-2,4,6-triethylbenzene (Scheme 1, A) (2.0g, 4.6mmol) in 20mL of anhydrous THF. The mixture was stirred for 5h. Then the mixture was combined with 50mL of ultrapure water and extracted three times with 50mL $CHCl_3$. The organic phases were added up and dried over $MgSO_4$ and the solvent was removed under reduced pressure. The solid was washed with diethyl ether and dried in vacuum.

The product was obtained as colorless crystals in a yield of 63%. It was characterized by ^{1}H-NMR and ^{13}C-NMR. ^{1}H-NMR ($CDCl_3$, 300 MHz): δ: 0.83 (9H, t, Me), 2.14 (9H, s, Me), 2.15 (9H, s, Me), 2.65 (6H, q, CH_2), 5.17 (6H, s, CH_2), 5.78 (3H, s, pyrazol-4-yl-H); ^{13}C-NMR ($CDCl_3$, 300 MHz): δ:12.4 (3C, s, Me), 13.65 (3C, s, Me), 15.31 (3C, s, Me), 24.12 (3C, s, CH_2), 106.03 (3C, s, pyrazol-4-yl-H), 139.85 (3C, s, N-C=CH_2), 145.62 (3C, s, benzene-Et), 147.38 (3C, s, N=C-CH_3). The spectra are comparable to previous literature on the synthesis of this tripodal ionophore [26-28].

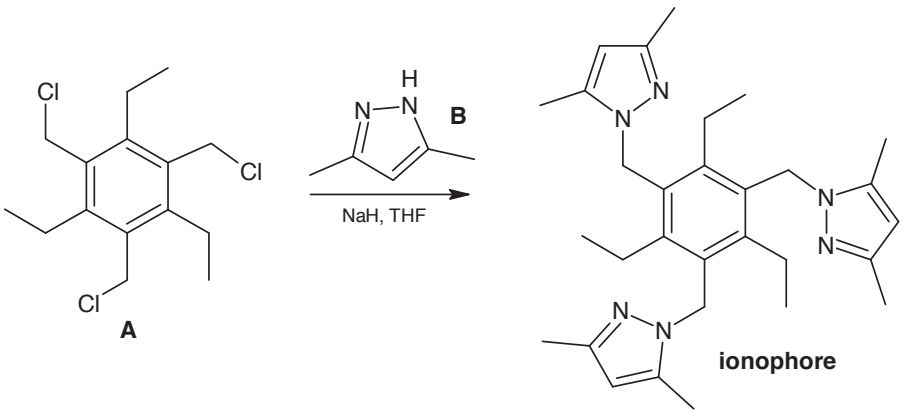

Scheme 1. Synthetic route of the ammonium-selective tripodal ionophore.

5.2.3 Membrane preparation

Membranes were prepared following the procedure reported by Schow *et al.* [19] and Sugiura *et al.* [32]. Different proportions of PVC (25.0g·L^{-1}) in THF, ionophore and DEHP (without further dilution), were used to produce membranes with a total weight of 0.6g excluding the solvent. The corresponding mixture of each membrane was placed in a 9cm diameter flat bottom glass Petri-dish. The dish was put in a flat box under nitrogen atmosphere for 72h to allow the solvent to evaporate slowly and have little contact with air humidity, thus to avoid formation of pores. Then, membranes were peeled off the dish by adding a few droplets of ultrapure water.

5.2.4 Membrane characterization

Thickness and swelling degree

A thickness gauge was used to measure the average thickness of each of the membranes. The swelling degree (sd)(-) (%) of the produced membranes was determined by the water uptake of a piece of dry membrane (20cm^2) with an identified mass. Three pieces of each of the membrane compositions were used to calculate the average swelling degree. It was calculated according to equation (1):

$$sd\ (\%) = \frac{m_{wet} - m_{dry}}{m_{dry}} x100 \qquad (1)$$

where m_{dry} and m_{wet} are the mass of the dry membrane and the mass of the swollen membrane (water uptake) after 24h in a water bath at room temperature, respectively. Before weighing m_{wet}, an adsorbent paper was used to remove the water film around the PIM.

Cation uptake in the membrane

The amount of each of the cations in the bulk of the membrane was determined by mass balance [33]. A piece of each of the produced membranes of 63.6cm^2 was put in contact with 150mL of a salt mixed solution of 0.33M of NH_4NO_3, KNO_3 and $NaNO_3$ making the ionic strength similar to the single salt solutions at 0.1M. After 120h, the membrane was wiped with an adsorbent paper and placed in 50mL of ultrapure water for 24h. The cation uptake is the amount of each of the cations released in the water per content of ionophore present in the membrane. For the membranes containing no ionophore, no cation uptake was observed. The relative cation uptake was calculated as the proportion between the amount of NH_4^+ uptaken and the other competitive ion (Na^+ or K^+).

Morphology

Scanning Electron Microscope (SEM) analysis was carried out to visualize the cross-sectional and perpendicular areas of the produced PIMs. Membranes were submerged in liquid nitrogen and fractured for neat observations. A gold spatter coating was applied on the membranes using a Jeol JFC-1200 Fine Coater (The Netherlands) and membranes were scanned by a Jeol JSM-6480LV Scanning Electron Microscope (The Netherlands).

Transport experiments

To assess the transport of ions, synthesized PIMs were clamped between the two compartments of a diffusion cell (Figure 1). The diffusion cell was made of poly(methyl) acrylate (PMMA) and consisted of two compartments between which the PIMs were clamped on a Teflon ring-shaped support. PIMs under study had a working area of 7.07cm^2. For reference, the side of the membrane exposed to the nitrogen atmosphere was placed facing the receiving compartment. Each of the compartments of the diffusion cell had a capacity of 100mL and phases were homogenized by stirring at a speed of 500rpm with magnetic bars. The feed compartment was filled with 0.1M aqueous solutions containing the nitrate salts, and the receiving compartment was filled with ultrapure water. All measurements were carried out at room temperature.

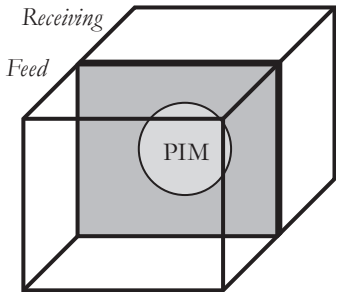

Figure 1. Scheme of the diffusion cell.

Samples of 1mL were taken from each compartment at different time intervals. The volume difference was compensated by adding 1mL of ultrapure water in the corresponding compartment after every sample. Because of the addition of ultrapure water, a dilution is induced in the phases and this was taken into account during calculations.

Flux J_i (mmol $cm^{-2}h^{-1}$) across the membranes for each of the ions was calculated as shown in equation (2):

$$J_i = \frac{V}{A}\frac{dC_i}{dt} \qquad (2)$$

where V (L) is the volume of the compartment, A (cm^2) is the membrane working area and $\frac{dC_i}{dt}$ ($mmol_i\ L^{-1}\cdot h^{-1}$) is the concentration change in time.

The relative selectivity between two different ions ($\alpha_{i,j}$) (-) was calculated as shown in equation (3):

$$\alpha_{i,j} = \frac{J_i}{J_j}\frac{\Delta C_j}{\Delta C_i} \qquad (3)$$

where $\Delta C_{i,j}$ is the concentration difference of each of the ions (i and j) at the end of the experiment.

5.2.5 Analyses

The chemical structure of the ionophore was determined by ^1H- and ^{13}C-NMR spectra recorded on a Varian VXR spectrometer (300MHz), using $CDCl_3$ as solvent. The reported chemical shifts were referenced to the resonances of the residual solvent or tetramethylsilane (TMS).

Ionophore and the produced membranes were characterized by Attenuated Total Reflection-Fourier Transform Infrared (ATR-FTIR) by a Bruker IFS88 FT-IR spectrometer. For each sample, 16 scans were performed.

The influence of each component of the membrane on the chemical functionality of the other components was determined by thermal analysis. Thermal transitions were measured by Differential Scanning Calorimetry (DSC) on a TA-Instruments Q1000. The heating and cooling rates were 10 °C·min^{-1}. Thermal stability was characterized by thermal gravimetric analysis (TGA) on a PerkinElmer thermogravimetric analyzer TGA7 under nitrogen environment. The scan rate was 10 °C·min^{-1}.

To determine the mass balance, the concentration of K^+, Na^+ and $NH_4^+$was determined by ion-chromatography (IC, Metrohm Compact, IC 761).

5.3 Results and discussion

The tripodal ionophore based on tripodal pyrazole substituted benzene was successfully synthesized according to Scheme 1 in sufficient quantities to study its ammonium selectivity in PIMs that could be readily produced.

Kim *et al.* [26] have shown via computational studies that the ammonium selectivity of the ionophore used is based on a delicate interplay of the three pyrazole nitrogen atoms and the NH_4^+ as in the ionophore they are ideally positioned for hydrogen bonding to NH_4^+ with $N_R\cdots N_A$ distances of about 3Å and $N_R\cdots N_A\cdots N_R$ angles of about 110° (where N_R represents the imine nitrogen atom and N_A represents the NH_4^+ nitrogen atom). It is therefore of utmost importance to study whether hydrogen bonding or ionic interactions between the ionophore and the other components in the produced PIMs (PVC and DEHP) can be observed. This could possibly influence the selectivity of the ionophore.

Furthermore, each of the components of the PIM can have an effect on the membrane characteristics and we therefore characterized the ionophore and investigated the composition of the membrane by means of structural analysis (ATR-FTIR and thermal analysis) and of cation transport and selectivity.

5.3.1 Composition and thermal analysis of PIMs

An assessment of possible hydrogen or ionic bonding of the plasticizer (DEHP), the polymer (PVC) on the tripodal ionophore when combined in the membrane matrix was carried out by FTIR analysis – a technique that is very sensitive for these interactions. The effect on the degradation of each of the components was assessed by thermogravimetric analysis (TGA) and thermal properties by differential scanning calorimetry (DSC).

FTIR characterization

FTIR analysis of each of the components and the membranes was carried out. Figure 2 shows the spectra of the pristine components of the membrane before producing the membrane. Figure 3 shows the spectra of the produced PIMs to evaluate the formation of hydrogen or ionic bonds during or after the production of the membranes. It can be clearly seen that formation of the membrane containing only PVC did not alter the chemical structure of the polymer, as Figure 2 (PVC) and Figure 3 (membrane 100 wt.% PVC) are identical spectra. Furthermore, after addition of DEHP and the ionophore in the membrane matrix (Figure 3, DEHP:PVC 1:3 and 5 wt.% ionophore) no additional FTIR bands can be observed. This indicates clearly that no hydrogen or ionic bonding between all three components is formed and therefore neither the 3-dimensional structure nor the energetic levels of the ionophore are altered. The ionophore should therefore still show the same selectivity as in its pristine state.

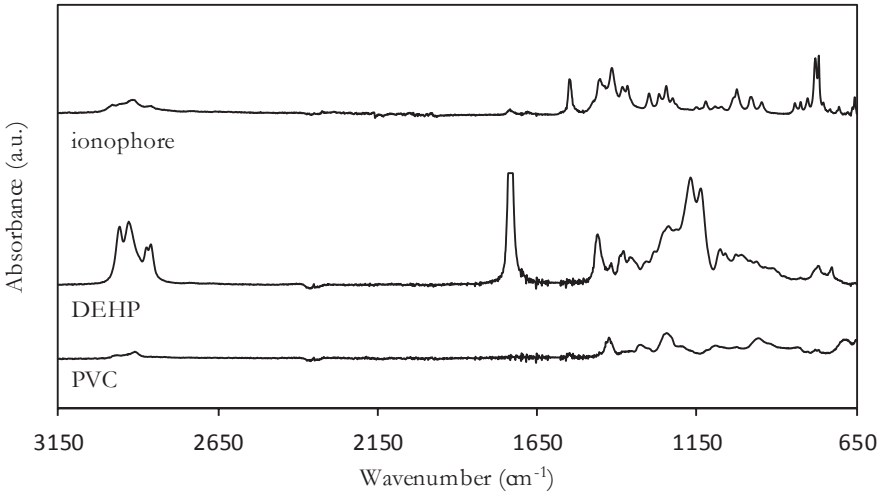

Figure 2. FTIR spectra of pristine PVC, DEHP and ionophore before producing the PIMs.

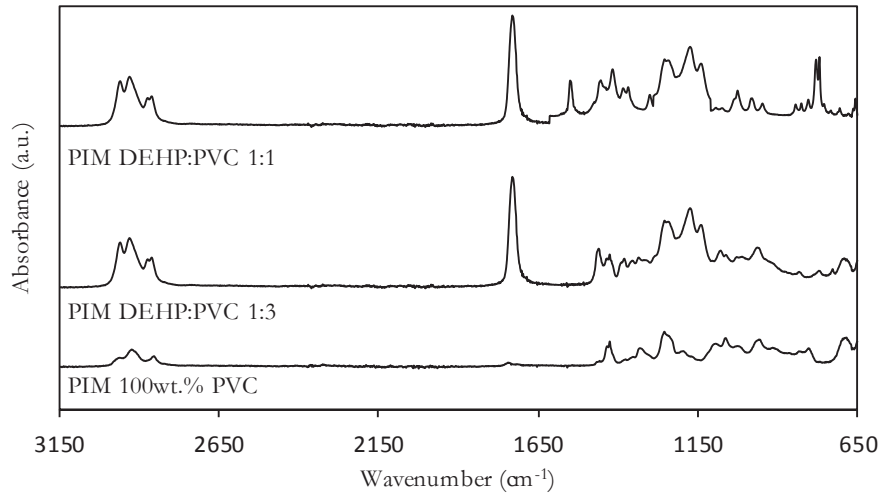

Figure 3. FTIR spectra of the produced PIMs.

Thermal analysis

Figure 4 shows the degradation steps of PIMs containing PVC only (a) and 2 different contents of DEHP:PVC (1:3 (b) and 1:1 (c)). The thermodegradation of PVC presents an initial step losing ~7wt.% corresponding to the evaporation of traces of solvent (THF) and possibly water. The second degradation step of PVC (a) is related to the release of HCl (~55 wt.%) and the third corresponds to degradation of the C-C bonds of the polymer backbone (~26 wt.%) [34]. The plasticized membranes present two main degradation steps, similar to PVC. The degradation steps for membranes composed of DEHP:PVC 1:3 (b) and 1:1 (c) present a higher weight loss during the first degradation: ~70wt.% (b) and ~79wt.% (c) than the degradation of the membrane containing only PVC (~55 wt.%). The higher the content of plasticizer present in the membrane, the easier is the release of HCl and therefore the onset is at lower temperatures (c) than (b) and (a). This is due to the free volume induced by DEHP that allows more efficient release of HCl [35]. The plasticizer penetrates among the polymer molecules and reduces the intermolecular forces of the polymer by increasing the distance between polymer molecules [17]. However, the difference (~9wt.%) in weight loss for (b) and (c) are not proportional to the addition of plasticizer (~17wt.%). This can be attributed to the fact that both membranes (b) and (c) also show an additional weight loss of ~10 wt.% at the degradation point of DEHP (around 323 ºC [35]) which explains this discrepancy.

The last degradation step, as in PVC, represents the degradation of C-C to compounds of lower molecular weight and to the production of additional volatile compounds. The remaining weight for the membrane containing 100wt.% PVC is ~26 wt.% and the content is reduced for both plasticized membranes to ~16 wt.%. The difference is related to the loss of the plasticizer in the previous steps.

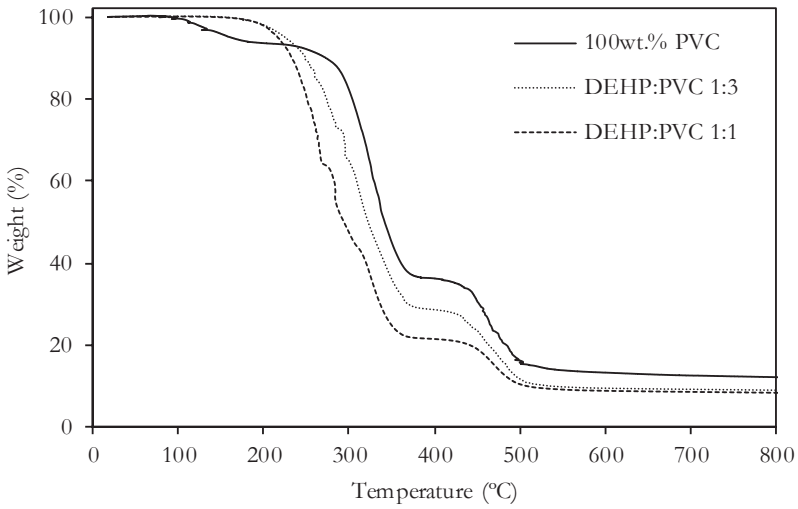

Figure 4. TGA traces of produced PIMs containing different contents of polymer (PVC) and plasticizer (DEHP).

Figure 5 shows the effect of the addition of ionophore 2wt.% and 5wt.% ((d) and (e), (f) and (g)) on the degradation of PIMs containing 2 different contents of DEHP:PVC (1:3 (b) and 1:1 (c)). In both cases (1:3 and 1:1), the addition of the ionophore lowers the degradation temperature of the membrane matrix when compared to the plasticized only membranes (b) and (c) suggesting an effect of the degradation of the ionophore. In general, for both cases (1:3 and 1:1) the addition of ionophore results in a lower weight loss in the first degradation step but higher in the second one as the remaining weight is similar for membranes with and without ionophore. This suggests that the ionophore occupies the free space provided by the DEHP and hampers the release of HCl from the degradation of PVC. The content of ionophore (2wt.% or 5wt.%) presents a difference (~4 wt.%) in the weight loss of the plasticized membrane 1:3 ((d) and (e)). This suggests that the ionophore degrades together with the PVC and DEHP in the first degradation step in concordance with the difference in the degradation temperature in the same degradation step. This

effect is not visible for membranes plasticized 1:1 ((g) and (f)) because the effect of the plasticizer is more relevant.

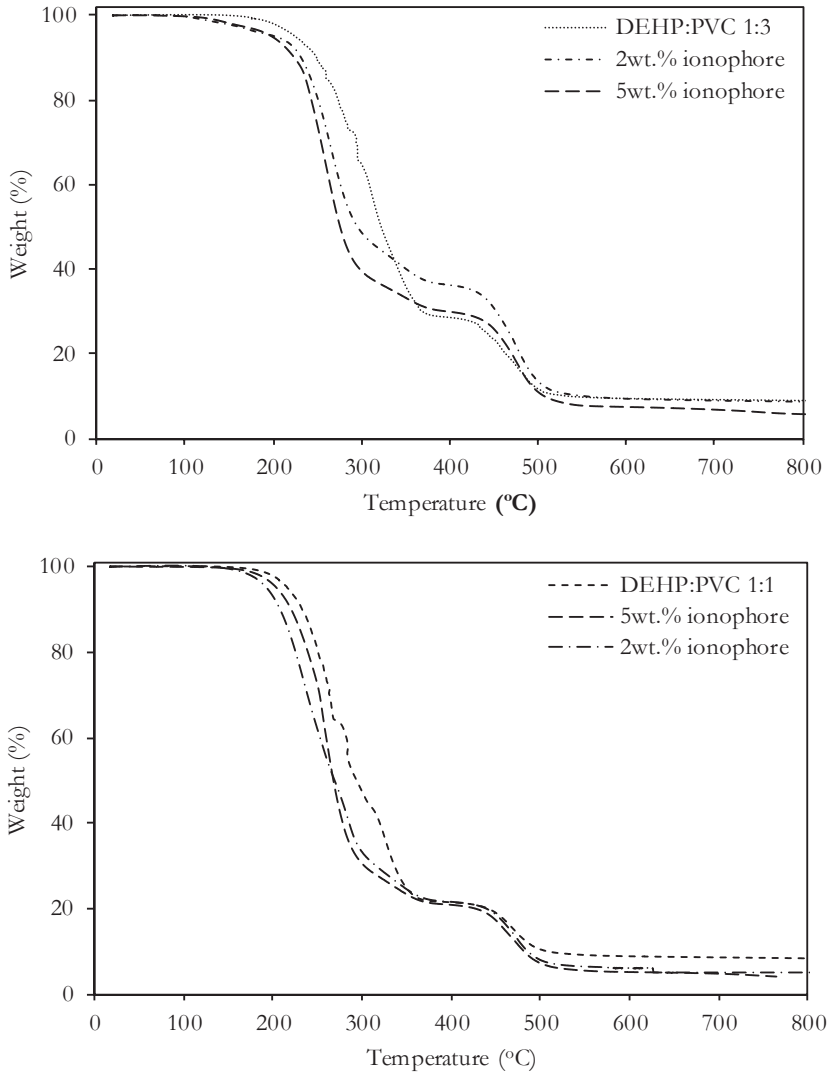

Figure 5. TGA traces of produced PIMs containing different contents of polymer (PVC), plasticizer (DEHP) and ionophore.

The same trend can be observed for the change of the glass transition temperature (T_g) depending on the composition of the membrane (Table 1). The higher the content of plasticizer, the lower the T_g. This is due to the fact that DEHP increases the distance between the polymer molecules and the T_g is reached at lower temperatures [36]. The addition of the ionophore, as already observed in TGA, hampers the effect of the plasticizer and the T_g increases again reaching about the same T_g as the membrane containing only PVC.

Table 1. Glass transition temperatures (T_g) of the synthesized membranes.

Composition	ionophore (wt. %)	T_g (°C)
100 wt.% PVC	0.0	63.1
DEHP:PVC 1:1	0.0	27.0
DEHP:PVC 1:1	2.0	57.3
DEHP:PVC 1:1	5.0	55.8
DEHP:PVC 1:3	0.0	43.5
DEHP:PVC 1:3	2.0	64.4
DEHP:PVC 1:3	5.0	65.0

Chemical structure determination and thermal analysis indicate that PVC, DEHP and the ionophore interact on a physical structural level but no hydrogen or ionic bonds between the components in the PIM are formed. However, the best composition for the recovery of NH_4^+ in the presence of the competitive ions (Na^+ and K^+) needs to be tested for its transport and selective properties.

5.3.2 Transport and selectivity

Thickness and Morphology

Table 2 gives an overview of the membranes produced in regard of their composition and thickness. PIMs with the same loadings of DEHP and PVC as the ones used in ISE literature with the same ionophore [27] were not successfully produced as they resulted in a very low viscosity. The resulting membrane presented a too high viscosity to be manipulated. Thus, membranes with lower loadings of DEHP were produced. PIMs had a thickness around 90μm except when the addition of the ionophore was 5wt.% where PIMs had a thickness around 100μm. Ionophore precipitated in the membrane matrix when its loading was above 5wt.%.

Table 2. Composition and thickness of the produced membranes and the ISE produced in literature (n.a. = not applicable).

#	Ionophore (wt. %)	DEHP:PVC (-)	Thickness (μm)
ISE [27]	1.0	2:1	n.a.
1	0.0	2:1	n.a.
2	0.0	0.0	92±11
3	0.0	1:1	89±13
4	2.0	1:1	88±6.6
5	5.0	1:1	98±5.3
6	0.0	0.3	84±10
7	2.0	0.3	82±8.9
8	5.0	0.3	97±5.5

To identify the morphology of the membranes, SEM images were taken for a PIM containing only PVC – Figure 6, a), DEHP:PVC 1:3 b) and DEHP:PVC 1:3 with 5wt.% of ionophore c). The three membranes are mainly dense and homogeneous with few micropores in their structure. The addition of plasticizer (Figure 6, b) and c)) resulted in a matrix of the membrane visually smoother than the one containing only PVC (a). This is in accordance with the reduction of the brittleness the plasticizer provides to PVC. There is no evidence that the ionophore crystallized in the membrane matrix (c) as no crystals were observed for this ionophore loading.

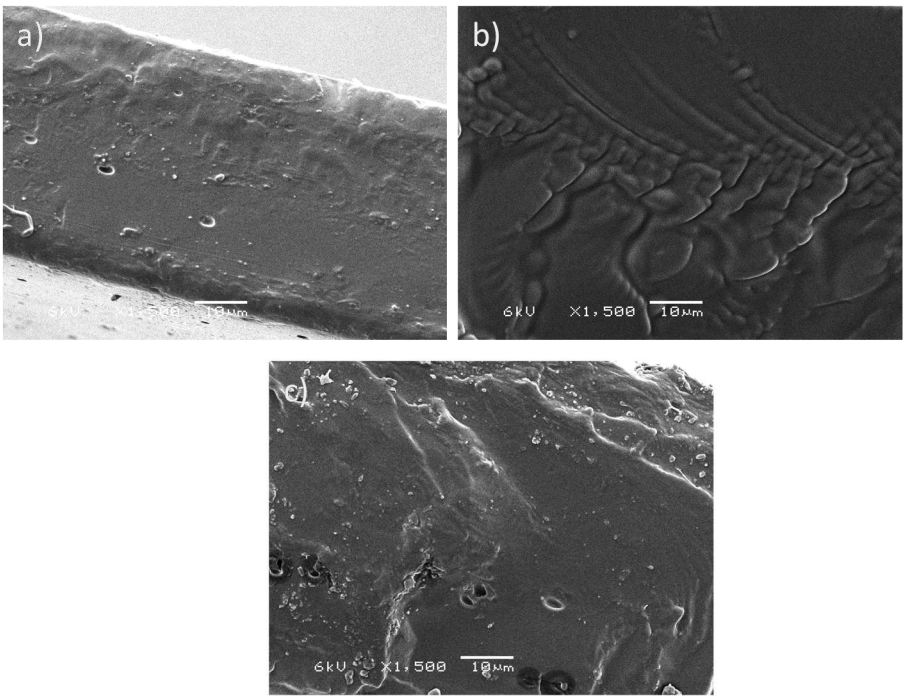

Figure 6. SEM images of the synthesized membranes: a) 100 wt.% PVC, b) DEHP:PVC 1:3 c) DEHP:PVC 1:3 with 5 wt.% of ionophore.

Swelling degree and cation uptake in the membrane

For the successful ion transport in a membrane an electrical diffusion layer (EDL) is required to overcome the resistance the membrane presents [37]. Therefore, we studied the ability of the produced PIMs to uptake water and the cations that go along in a salted solution (swelling degree, sd) in their structure. Table 3 indicates that the plasticizer reduces the water uptake in the membrane due to its high hydrophobicity. Loadings of 1:1 of DEHP:PVC resulted in a sd between 1-2% whilst loadings of 1:3 (1:3 DEHP:PVC) resulted in a sd between 3.5-6.7%. Thus membranes with a lower loading of DEHP:PVC are more prone to have higher ion fluxes.

Table 3. Swelling degree of the produced PIMs.

#	ionophore (wt. %)	DEHP:PVC (-)	sd (-) (%)
4	2.0	1:1	1.58±1.7
5	5.0	1:1	2.16±0.8
7	2.0	1:3	3.45±0.9
8	5.0	1:3	6.67±1.2

The addition of ionophore plays an important role on the ion flux especially on the selectivity of the membranes as well. Table 4 presents the selectivity given by the relative cation uptake of the bulk membrane. When the content of ionophore is 2wt.% (#4 and #7) the cation uptake is higher in comparison to the content of ionophore being 5wt.% (#5 and #8). These observations are consistent with the swelling degree results in Table 3. In addition, the relative cation uptake shows a higher selectivity of the membranes with higher loading

of ionophore in their matrix. Our hypothesis is that uptake and selectivity are higher due to the higher percolation of ions into the bulk of the membrane.

Table 4. Cation uptake in the bulk of the membrane for NH_4^+, Na^+ and K^+.

#	*Cation uptake* ($mmol_i \cdot mmol_{ionophore}^{-1}$)			*Relative Cation uptake* (-)	
	NH_4^+	**Na^+**	**K^+**	**NH_4,Na**	**NH_4,K**
4	0.59	0.19	0.21	3.10	2.81
5	0.42	0.27	0.24	1.56	1.75
7	0.64	0.12	0.12	5.31	5.33
8	0.47	0.22	0.25	2.14	1.88

Transport and selectivity

As expected membranes without ionophore present no selectivity; NH_4^+, Na^+ and K^+ show similar fluxes in each membrane (Table 5) after 120h. Addition of plasticizer results in a difference among the three produced membranes without ionophore. In membranes without plasticizer (100 wt.% PVC) the flux for single salts transport is around 5.0 $x10^{-3}$ $mmol \cdot cm^{-2} \cdot h^{-1}$ whilst for membranes containing the same content (weight) of plasticizer and polymer (DEHP:PVC 1:1) the flux is very close to zero. This is due to the hydrophobicity of the plasticizer that does not provide affinity of the solvated ions with the membrane.

However, when the content of plasticizer and polymer are 1:3 the flux increases and becomes higher (7.5 $x10^{-3}$ $mmol \cdot cm^{-2} \cdot h^{-1}$) than for the membrane containing no plasticizer (5.0 $x10^{-3}$ $mmol \cdot cm^{-2} \cdot h^{-1}$). This is consistent with the results observed in the thermogravimetric measurements (Figure 4). The

presence of plasticizer reduces the intermolecular forces of the PVC structure and the membrane becomes less rigid so cations can be transported across.

Table 5. Cation flux of produced membranes without ionophore in single and mixed salt solutions.

Composition	*single salt transport* (x10^{-3} mmol·cm^{-2}·h^{-1})			*mixed salts transport* (x10^{-3} mmol·cm^{-2}·h^{-1})		
	J_{NH4}	J_{Na}	J_K	J_{NH4}	J_{Na}	J_K
100wt.% PVC	4.91	4.96	5.02	1.47	1.72	1.72
DEHP:PVC 1:1	0.06	0.08	0.08	0.02	0.02	0.02
DEHP:PVC 1:3	7.49	7.47	7.48	2.61	2.59	2.61

Given the high flux of the membrane containing DEHP:PVC 1:3, membranes with ionophore were produced with this loading of DEHP:PVC. Experiments were carried out during 120h, with a concentration of NH_4^+ in the receiving compartment being half the initial concentration (equilibrium). Although fluxes are lower than for the membranes without ionophore (<7.5 x10^{-3} mmol·cm^{-2}·h^{-1}), they present selectivity of NH_4^+ over Na^+ and K^+ (Table 6). The flux of NH_4^+ increases as the content of ionophore increases. For single salt transport, when the content of ionophore is 2wt.%, the flux is 3.68 x10^{-3} mmol·cm^{-2}·h^{-1} whilst when it is 5wt.%, the flux is 5.17x10^{-3} mmol·cm^{-2}·h^{-1}. This is due to the transport mechanism of the cations in the bulk of the membrane: the jumping mechanism [38]. Cations are percolated across the membrane by jumping from one ionophore to another, driven by the concentration gradient. Therefore, the more ionophore, the more efficient the percolation is. A possible approach to increase the flux across the membrane could be with the addition of an anionic additive into the membrane matrix such as tetrakis(*p*-chlorophenyl) borate [27-28]. However, further research needs to be carried out as Suzuki *et al.* [23] did not add the lipophilic anion and achieved similar results.

However, selectivity is affected by greater fluxes and in this study, selectivity was studied for mixed salts transport. When the content of ionophore is 2wt.%, selectivity of NH_4^+ over Na^+ is around 13.07 and over K^+ it is 14.15 whilst when it is 5wt.%, the selectivity over Na^+ is 9.33 and over K^+ is 9.57. No selectivity of K^+ over Na^+ can be observed in any of the produced membranes. The selectivity of the ionophore in ISEs was reported to be 100 times higher [23, 27, 28]. This is attributed to the higher contact of the solution with the membrane in an ISE set-up (Table 3) and the effect of the concentration gradient across the membrane gains more importance [39].

Table 6. Cation flux and selectivity of produced membranes (DEHP:PVC 1:3) containing ionophore in single and mixed salt solutions.

Composition	*single salt transport* ($x10^{-3}$ mmol·cm^{-2}·h^{-1})			*mixed salts transport* ($x10^{-3}$ mmol·cm^{-2}·h^{-1})				
	J_{NH4}	J_{Na}	J_K	J_{NH4}	J_{Na}	J_K	$\alpha_{NH4/Na}$ (-)	$\alpha_{NH4/K}$ (-)
2 wt.%	3.68	3.00	3.08	3.34	1.86	1.72	13.07	14.15
5wt.%	5.17	3.83	3.68	4.86	2.60	2.54	9.33	9.57

5.4 Conclusions

A membrane selective for ammonium was successfully produced and the factors rendering its performance were investigated. FTIR, TGA and DSC measurements showed that the plasticizer reduces the rigidity of the membranes by reducing the intermolecular forces among the polymer chains. No new hydrogen or ionic bonds between the three components of the PIM were formed that could influence the selectivity of the successfully synthesized tripodal ionophore based on pyrazole substituted benzene. The addition of ionophore increased the swelling degree of the PIM and therefore the affinity

of the cations to the membrane. Two different contents of plasticizer were tested DEHP:PVC 1:1 and DEHP:PVC 1:3. The latter content was the one used for transport and selectivity characterization due to its higher hydrophobicity.

The two tested contents of ionophores (2 and 5 wt.%) showed that the higher the content of ionophore in the membrane matrix, the faster the flux. However, selectivity is reduced. When the content of ionophore is 2wt.%, selectivity of NH_4^+ over Na^+ is around 13.07 and over K^+ it is 14.15 whilst when it is 5wt.%, the selectivity over Na^+ is 9.33 and over K^+ is 9.57. No selectivity of K^+ over Na^+ can be observed. This study shows that the use of the tripodal ionophore is a good approach for the development of ammonium-selective membranes. Further investigation needs to be conducted to increase the fluxes of the transported cations as well as the ionophore selectivity in high fluxes.

5.5 References

1. FAO, Global agriculture towards 2050, in, Food and Agriculture Organization of the United Nations, Rome, 2009.

2. S. Zhang, C.Y. Lim, C.-L. Chen, H. Liu, J.-Y. Wang, Urban nutrient recovery from fresh human urine through cultivation of Chlorella sorokiniana, Journal of Environmental Management, 145 (2014) 129-136.

3. M. Kitano, Y. Inoue, Y. Yamazaki, F. Hayashi, S. Kanbara, S. Matsuishi, T. Yokoyama, S.W. Kim, M. Hara, H. Hosono, Ammonia synthesis using a stable electride as an electron donor and reversible hydrogen store, Nature Chemistry, 4 (2012) 934-940.

4. K.M. Udert, M. Wächter, Complete nutrient recovery from source-separated urine by nitrification and distillation, Water Research, 46 (2012) 453-464.

5. J.A. O'Neal, T.H. Boyer, Phosphate recovery using hybrid anion exchange: Applications to source-separated urine and combined wastewater streams, Water Research, 47 (2013) 5003-5017.

6. R.C. Tice, Y. Kim, Energy efficient reconcentration of diluted human urine using ion exchange membranes in bioelectrochemical systems, Water Research, 64 (2014) 61-72.

7. K. Diem, C. Lentner, Documenta Geigy: Scientific tables, 7 ed., Georg Thieme Verlag Stuttgart, 1975.

8. P. Kuntke, T.H.J.A. Sleutels, M. Saakes, C.J.N. Buisman, Hydrogen production and ammonium recovery from urine by a Microbial Electrolysis Cell, International Journal of Hydrogen Energy, 39 (2014) 4771-4778.

9. P. Kuntke, K. Śmiech, H. Bruning, G. Zeeman, M. Saakes, T. Sleutels, H. Hamelers, C. Buisman, Ammonium recovery and energy production from urine by a microbial fuel cell, Water Research, 46 (2012) 2627-2636.

10. M. Maurer, P. Schwegler, T.A. Larsen, Nutrients in urine: energetic aspects of removal and recovery, Water Science and Technology, 48 (2003) 37-46.

11. D.R. Lide, Handbook of Chemistry and Physics, 85 ed., CRC Press, 2004.

12. E.R. Nightingale, Phenomenological Theory of Ion Solvation. Effective Radii of Hydrated Ions, The Journal of Physical Chemistry, 63 (1959) 1381-1387.

13. J.P. Shukla, A. Kumar, R.K. Singh, Macrocycle-mediated selective transport of plutonium(IV) nitrate through bulk liquid and supported liquid membranes using

dicyclohexano-18-crown-6 as mobile carrier, Separation Science and Technology, 27 (1992) 447-465.

14. J. Tomar, A. Awasthy, U. Sharma, Synthetic ionophores for the separation of Li^+, Na^+, K^+, Ca^{2+}, Mg^{2+} metal ions using liquid membrane technology, Desalination, 232 (2008) 102-109.

15. N.E. Belkhouche, M.A. Didi, R. Romero, J.A. Jönsson, D. Villemin, Study of new organophosphorus derivates carriers on the selective recovery of M (II) and M (III) metals, using supported liquid membrane extraction, Journal of Membrane Science, 284 (2006) 398-405.

16. S.S. Madaeni, H.R.K. Zand, Selective transport of bismuth ions through supported liquid membrane, Chemical Engineering and Technology, 28 (2005) 892-898.

17. L.D. Nghiem, P. Mornane, I.D. Potter, J.M. Perera, R.W. Cattrall, S.D. Kolev, Extraction and transport of metal ions and small organic compounds using polymer inclusion membranes (PIMs), Journal of Membrane Science, 281 (2006) 7-41.

18. M.I.G.S. Almeida, R.W. Cattrall, S.D. Kolev, Recent trends in extraction and transport of metal ions using polymer inclusion membranes (PIMs), Journal of Membrane Science, 415–416 (2012) 9-23.

19. A.J. Schow, R.T. Peterson, J.D. Lamb, Polymer inclusion membranes containing macrocyclic carriers for use in cation separations, Journal of Membrane Science, 111 (1996) 291-295.

20. P. Bühlmann, E. Pretsch, E. Bakker, Carrier-Based Ion-Selective Electrodes and Bulk Optodes. 2. Ionophores for Potentiometric and Optical Sensors, Chemical Reviews, 98 (1998) 1593-1688.

21. E. Bakker, P. Bühlmann, E. Pretsch, Carrier-Based Ion-Selective Electrodes and Bulk Optodes. 1. General Characteristics, Chemical Reviews, 97 (1997) 3083-3132.

22. S. Chandra, R. Buschbeck, H. Lang, A 15-crown-5-functionalized carbosilane dendrimer as ionophore for ammonium selective electrodes, Talanta, 70 (2006) 1087-1093.

23. K. Suzuki, D. Siswanta, T. Otsuka, T. Amano, T. Ikeda, H. Hisamoto, R. Yoshihara, S. Ohba, Design and Synthesis of a More Highly Selective Ammonium Ionophore Than Nonactin and Its Application as an Ion-Sensing Component for an Ion-Selective Electrode, Analytical Chemistry, 72 (2000) 2200-2205.

24. R.M. Izatt, B.L. Nielsen, J.J. Christensen, J.D. Lamb, Membrane transport of ammonium and alkylammonium cations using macrocyclic carriers, Journal of Membrane Science, 9 (1981) 263-271.

25. E. Graf, J.P. Kintzinger, J.M. Lehn, J. LeMoigne, Molecular recognition. Selective ammonium cryptates of synthetic receptor molecules possessing a tetrahedral recognition site, Journal of the American Chemical Society, 104 (1982) 1672-1678.

26. J. Chin, C. Walsdorff, B. Stranix, J. Oh, H.J. Chung, S.-M. Park, K. Kim, A Rational Approach to Selective Recognition of NH4+ over K+ Angewandte Chemie International Edition, 38 (1999) 2756-2759.

27. J. Chin, J. Oh, S.Y. Jon, S.H. Park, C. Walsdorff, B. Stranix, A. Ghoussoub, S.J. Lee, H.J. Chung, S.-M. Park, K. Kim, Tuning and Dissecting Electronic and Steric Effects in Ammonium Receptors: Nonactin vs Artificial Receptors, Journal of the American Chemical Society, 124 (2002) 5374-5379.

28. S.-i. Sasaki, T. Amano, G. Monma, T. Otsuka, N. Iwasawa, D. Citterio, H. Hisamoto, K. Suzuki, Comparison of Two Molecular Design Strategies for the Development of an Ammonium Ionophore More Highly Selective than Nonactin, Analytical Chemistry, 74 (2002) 4845-4848.

29. H.-S. Kim, H.J. Park, H.J. Oh, Y.K. Koh, J.-H. Choi, D.-H. Lee, G.S. Cha, H. Nam, Thiazole-Containing Benzo-Crown Ethers: A New Class of Ammonium-Selective Ionophores, Analytical Chemistry, 72 (2000) 4683-4688.

30. J.S. Benco, H.A. Nienaber, W.G. McGimpsey, Synthesis of an Ammonium Ionophore and Its Application in a Planar Ion-Selective Electrode, Analytical Chemistry, 75 (2002) 152-156.

31. W.G. McGimpsey, E. Soto, P.F. Driscoll, C. Nowak, J.S. Benco, C.G.F. Cooper, C.R. Lambert, 13C NMR study of the ion-binding selectivity of a new ammonium ionophore, Magnetic Resonance in Chemistry, 46 (2008) 955-961.

32. M. Sugiura, M. Kikkawa, S. Urita, Carrier-mediated transport of rare earth ions through cellulose triacetate membranes, Journal of Membrane Science, 42 (1989) 47-55.

33. A.H. Galama, J.W. Post, M.A. Cohen Stuart, P.M. Biesheuvel, Validity of the Boltzmann equation to describe Donnan equilibrium at the membrane–solution interface, Journal of Membrane Science, 442 (2013) 131-139.

34. V. Krongauz, Y.-P. Lee, A. Bourassa, Kinetics of thermal degradation of poly(vinyl chloride), J Therm Anal Calorim, 106 (2011) 139-149.

35. Q.G. Aouachria K., Massardier-Nageotte V., Belhaneche-Bensemra, N., The effect of di-(-2-ethyl hexyl) phthalate (DEHP) as plasticizer on the thermal and mechanical properties of PVC/PMMA blends., Polímeros, 24 (2014) 428-433.

36. T.M. Martin, D.M. Young, Correlation of the glass transition temperature of plasticized PVC using a lattice fluid model, Polymer, 44 (2003) 4747-4754.

37. S. Sang, Q. Wu, K. Huang, A discussion on ion conductivity at cation exchange membrane/solution interface, Colloids and Surfaces A: Physicochemical and Engineering Aspects, 320 (2008) 43-48.

38. A. Gherrou, H. Kerdjoudj, R. Molinari, P. Seta, E. Drioli, Fixed sites plasticized cellulose triacetate membranes containing crown ethers for silver(I), copper(II) and gold(III) ions transport, Journal of Membrane Science, 228 (2004) 149-157.

39. A.H. Galama, J.W. Post, H.V.M. Hamelers, V.V. Nikonenko, M. Biesheuvel, On the origin of the membrane potential arising across densely charged ion exchange membranes: How well does the Teorell-Meyer-Sievers theory work?, Journal of Membrane Science and Research, (2015).